Inverse Heat Conduction in a Finite Slab with Measured Back Surface Temperature and Heat Flux

Jianhua Zhou[1], Yuwen Zhang[2], J. K. Chen[3], and Z. C. Feng[4]
University of Missouri, Columbia, MO 65211, USA

In High-Energy Laser (HEL) heating of target, the temperature and heat flux at the heated surface is not directly measurable, but can be estimated by solving an inverse heat conduction problem (IHCP) based on measured temperature or/and heat flux at the accessible (back) surface. In this study, the one-dimensional (1-D) IHCP in a finite slab is solved by the conjugate gradient method (CGM) using measured temperature and heat flux at the accessible (back) surface. Simulated measurement data are generated by solving a direct problem where the front surface of the slab is subjected to high intensity periodic heating. Two cases are simulated and compared, with the temperature or heat flux at the heated front surface chosen as the unknown function to be recovered. The results showed that the latter choice, i.e., choosing back surface heat flux as the unknown function, can give better estimation accuracy in the IHCP solution. The front surface temperature can be computed with a high precision as a byproduct of the IHCP algorithm. The robustness of this IHCP formulation is tested by different measurement errors and frequencies of the input periodic heating flux.

Nomenclature

c_p	=	specific heat
$d^k(t)$	=	direction of descent at iteration level k
h	=	convection heat transfer coefficient
k	=	thermal conductivity
L	=	thickness of 1-D slab
q''	=	intensity of heating source at front surface
$q_1(t)$	=	heat flux at front surface
$q[L,t;T_1(t)]$	=	computed heat flux at the back surface
S	=	objective functions
$\nabla S[T_1^k(t)]$	=	gradient direction of objective functional at iteration level k
$\Delta S[T_1(t)]$	=	objective function variation
t	=	time
t_f	=	final time
T	=	temperature
T_0	=	initial temperature
T_∞	=	ambient temperature
$T_1(t)$	=	front surface temperature
$T[L,t;T_1(t)]$	=	computed heat flux at the back surface
$\Delta T[x,t;T_1(t)]$	=	temperature variation
x	=	spatial coordinate variable

[1] Postdoctoral Research Associate, Department of Mechanical and Aerospace Engineering, AIAA Member.
[2] Associate Professor, Department of Mechanical and Aerospace Engineering, AIAA Associate Fellow.
[3] William and Nancy Thompson Professor, Department of Mechanical and Aerospace Engineering
[4] Professor and Director of Graduate Studies, Department of Mechanical and Aerospace Engineering

$Y(t)$ = measurement data (temperature or heat flux) with errors at back surface obtained by numerical simulations
$Y_{exact}(t)$ = measurement data (temperature or heat flux) without errors at back surface obtained by numerical simulations
$Y_{qL}(t)$ = measurement heat flux at the back surface
$Y_{TL}(t)$ = measurement temperature at the back surface

Greek symbols

β^k = search step size at iteration level k
χ = tolerance used to stop the CGM iteration procedure
δ = standard deviation of the measurements
ε = surface emissivity
γ^k = conjugate coefficient at iteration level k
$\lambda(x,t)$ = Lagrange multiplier
ρ = density
σ = Stefan-Boltzmann constant, $\sigma = 5.67 \times 10^{-8}$ W/(m^2 • K^4)
ω = random variable between 0 and 1

Superscripts

k = iteration level

Subscripts

0 = initial
f = final
q = heat flux
T = temperature

1. Introduction

High-Energy Laser (HEL) weapons offer the advantages of remote delivery at the speed of light onto a small spot on military target. During laser irradiation, it is critical to know the temperature at the heated front target surface in order to accurately understand damage mechanism. However, the heated front-surface is either inaccessible or too hot so that it is unsuitable for attaching a sensor. Similar problem can also be encountered in some laser manufacturing processes [1]. Under these circumstances, the front surface temperature can be determined indirectly by solving an inverse heat conduction problem [2-4] based on the transient temperature or/and heat flux measured at the back surface.

In the mathematical formulation of the inverse problem, either temperature or heat flux can be measured at the back surface. Most previous researchers prefer temperature measurements because temperature can be measured with fewer uncertainties compared to heat flux measurements [5-8]. However, recent studies have showed that using measured heat flux as additional information in the formulation of an IHCP can increase the stability of the solution and is less prone to the inherent instability of the ill-posed problem of inverse heat conduction [9, 10].

Although the inverse heat conduction problems have been extensively studied for different applications in the past (e.g., [11-19]), little work has been done for the inverse problem related to laser irradiation of a remote surface. The laser energy is delivered to the target surface in a periodic way because of laser or atmosphere variations. The periodic heat flux may pose extra difficulties in the solution of the inverse problems. Since the formulation of the IHCP is quite subjective, it is necessary to determine which formulation is most appropriate for these applications.

In this study, a 1-D inverse heat conduction problem in a finite slab is formulated and solved using the conjugate gradient method (CGM) with adjoint problem for function estimation [3, 4]. The inverse solutions for the cases where the front surface of the slab is subjected to high intensity periodic heating is illustrated to identify the most robust IHCP formulation for the laser manufacturing applications. Both the temperature and heat flux are measured at the back surface. The former is used as the back surface boundary condition while the latter is adopted in the objective function to be minimized. Two cases are examined in detail where the temperature or heat flux at the heated front surface is chosen as the unknown function to be recovered. The most robust and error-insensitive IHCP formulation will be proposed.

2. Model Description

For the case that the laser beam size is much larger than the thickness of the wall, one can treat the inverse heat transfer problem as one-dimensional. To illustrate the methodology of the inverse heat transfer algorithms used in this study, a finite slab with a thickness of *L*, as shown in Figure 1 is considered. Initially, the slab is uniformly at the temperature of T_0. From $t > 0$, the front surface of the slab is subjected to a high intensity laser heating. The purpose of the inverse problem is to reconstruct the heating condition at the front surface based on the measured temperature and heat flux at the back surface. Due to the fact that temperature measurement data contain much less errors compared to heat flux measurement [5-8], the temperature $Y_{TL}(t)$ is used as the boundary condition and the heat flux $Y_{qL}(t)$ is adopted in the objective function. It is assumed that the density, specific heat and the thermal conductivity of the slab are constants.

Two cases, i.e., Case I and Case II as shown in Fig. 1(a) and Fig. 1(b), respectively, are examined to test which quantity (temperature or heat flux) is more appropriate to be employed as the unknown to be recovered such that the best accuracy can be achieved.

In the following, the mathematical formulations for different cases will be described.

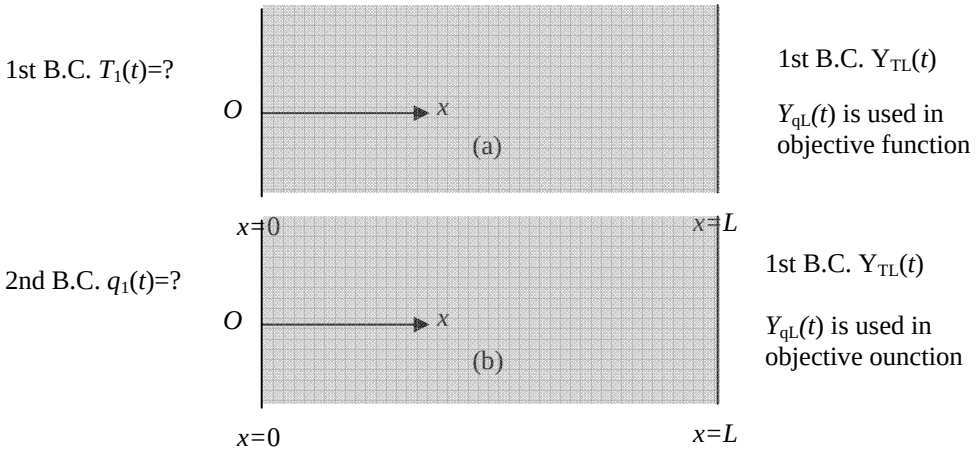

Figure 1 Physical models. (a) Case I: recovering the front-surface temperature $T_1(t)$. (b) Case II: recovering the front-surface heat flux $q_1(t)$.

2.1 The direct problem

2.1.1 Case I

For this case, the front surface temperature is chosen as the unknown to be recovered (Figure 1(a)). The direct problem for this case can be expressed as follows:

$$\rho c_p \frac{\partial T}{\partial t} = \frac{\partial}{\partial x}\left(k \frac{\partial T}{\partial x}\right) \qquad \text{in } 0 < x < L, \text{ for } t > 0 \qquad (1)$$

$$T(x,0) = T_0 \qquad \text{in } 0 < x < L, \text{ for } t = 0 \qquad (2)$$

$$T(x,0) = T_1(t) \qquad \text{at } x = 0, \text{ for } t > 0 \qquad (3)$$

$$T(L,t) = Y_{TL}(t) \qquad \text{at } x = L, \text{ for } t > 0 \qquad (4)$$

where $T_1(t)$ is the front surface temperature; $Y_{TL}(t)$ is the measuring temperature at the back surface.

In the direct problem associated with the physical problem described above, the front-surface temperature, $T_1(t)$, and the back surface temperature, $Y_{TL}(t)$, are considered to be known. The objective of the direct problem is then to determine the transient temperature distribution in the slab.

2.1.2 Case II

For this case, the front surface heat flux is chosen as the unknown to be recovered (Figure 1(b)). The mathematical formulations is almost the same as those in Eqs. (1) ~ (4) except that the boundary conditions at $x = 0$ is replaced by:

$$-k\frac{\partial T(0,t)}{\partial x} = q_1(t) \qquad \text{at } x = 0, \text{ for } t > 0 \tag{5}$$

where $q_1(t)$ is the front surface heat flux.

2.2 The inverse problem

For the inverse problem, the boundary condition at $x = 0$ is unknown, but everything else in the corresponding direct problem is known. The additional information needed in recovering the front surface boundary condition is available from the readings of a heat flux sensor installed at the back surface.

2.2.1 Case I

The inverse problem for this case can be expressed as follows:

$$\rho c_p \frac{\partial T}{\partial t} = \frac{\partial}{\partial x}\left(k\frac{\partial T}{\partial x}\right) \qquad \text{in } 0 < x < L, \text{ for } t > 0 \tag{6}$$

$$T(x,0) = T_0 \qquad \text{in } 0 < x < L, \text{ for } t = 0 \tag{7}$$

$$T(L,t) = Y_{TL}(t) \qquad \text{at } x = L, \text{ for } t > 0 \tag{8}$$

where the front surface temperature, $T_1(t)$, is regarded as unknown. The heat flux readings at the back surface, $Y_{qL}(t)$, are considered available as additional information.

The solution of the inverse problem will be obtained in such a way that the following objective function is minimized (for continuous measured data):

$$S[T_1(t)] = \int_0^{t_f} \{Y_{qL}(t) - q[L,t;T_1(t)]\}^2 dt \tag{9}$$

where $Y_{qL}(t)$ and $q[L,t;T_1(t)]$ are the measured and computed heat fluxes at the back surface, respectively.

2.2.2 Case II

The governing equations of the inverse problem for this case are the same as those in Case I (i.e., Eqs. (6) ~ (8)). The only difference is that the heat flux at the front surface, $q_1(t)$, is regarded as unknown and the following objective function is minimized:

$$S[q_1(t)] = \int_0^{t_f} \{Y_{qL}(t) - q[L,t;q_1(t)]\}^2 dt \tag{10}$$

2.3 Conjugate gradient method for minimization

The iterative process based on the CGM [3, 4] is now derived for the estimation of unknown temperature ($T_1(t)$) or heat flux ($q_1(t)$) by minimizing the objective function S.

The iterative process for Case I is as follows:

$$T_1^{k+1}(t) = T_1^k(t) - \beta^k d^k(t) \tag{11}$$

where β^k is the search step size in going from iteration k to iteration k+1, and $d^k(t)$ is the direction of descent (i.e. search direction) given by:

$$d^k(t) = \nabla S[T_1^k(t)] + \gamma^k d^{k-1}(t) \tag{12}$$

which is a conjugation of the gradient direction $\nabla S[T_1^k(t)]$ at iteration k and the direction of descent $d^{k-1}(t)$ at iteration k-1. The conjugate coefficient γ^k is determined from:

$$\gamma^k = \frac{\int_0^{t_f} \nabla S[T_1^k(t)] \cdot \{\nabla S[T_1^k(t)] - \nabla S[T_1^{k-1}(t)]\} dt}{\int_0^{t_f} \{\nabla S[T_1^{k-1}(t)]\}^2 dt} \quad \text{with } \gamma^0 = 0 \tag{13}$$

The iterative process for Case II can be obtained by replacing $T_1^{k-1}(t)$, $T_1^k(t)$ and $T_1^{k+1}(t)$ with $q_1^{k-1}(t)$, $q_1^k(t)$ and $q_1^{k+1}(t)$, respectively in Eqs. (11) ~ (13).

To perform the iterations according to Eq. (11), we need to compute the step size β^k and the gradient of the functional $\nabla S[T_1^k(t)]$. In order to develop expressions for the determination of these two quantities, a *sensitivity problem* and an *adjoint problem* for each case are constructed below.

2.4 Sensitivity problem and search step size

2.4.1 Case I

The sensitivity problem is obtained from the original direct problem (Eqs. (1) ~ (4) for Case I) in the following manner: It is assumed that when $T_1(t)$ undergoes a variation ΔT_1, T is perturbed by ΔT. Then replacing in the direct problem T_1 by $T_1 + \Delta T_1$ and T by $T + \Delta T$, subtracting from the resulting expressions the direct problem and neglecting the second-order terms, the sensitivity problem for the sensitivity function ΔT can be obtained.

The sensitivity problem for Case I can be expressed as:

$$\rho c_p \frac{\partial \Delta T}{\partial t} = \frac{\partial}{\partial x}\left(k \frac{\partial \Delta T}{\partial x}\right) \qquad \text{in } 0 < x < L, \text{ for } t > 0 \tag{14}$$

$$\Delta T(x,0) = 0 \qquad \text{in } 0 < x < L, \text{ for } t = 0 \tag{15}$$

$$\Delta T(0,t) = \Delta T_1(t) \qquad \text{at } x = 0, \text{ for } t > 0 \tag{16}$$

$$\Delta T(L,t) = 0 \qquad \text{at } x = L, \text{ for } t > 0 \tag{17}$$

The objective function for iteration k+1 is obtained by re-writing Eq. (9) as:

$$S[T_1^{k+1}(t)] = \int_0^{t_f} \{Y_{qL}(t) - q[L,t;(T_1^k - \beta^k d^k)]\}^2 dt \tag{18}$$

where T_1^{k+1} is replaced by the expression given by Eq. (11). If $q[L,t;(T_1^k - \beta^k d^k)]$ is linearized by a Taylor expansion, Eq. (18) takes the following form:

$$S[T_1^{k+1}(t)] = \int_0^{t_f} \{Y_{qL}(t) - q[L,t;T_1^k] - \beta^k \Delta q(d^k)\}^2 dt \tag{19}$$

where $q[L,t;T_1^k]$ is the solution of the direct problem (Eqs. (1) ~ (4)) by using estimated T_1^k at x=0 and time t. The sensitivity functions $\Delta q(d^k)$ are taken as the solutions of Eqs. (14) ~ (17) at the measured positions x=L and time t by letting $\Delta T_1 = d^k$. The search step size β^k is determined by minimizing the function given by Eq. (19) with respect to β^k. The following expression results:

$$\beta^k = \frac{\int_0^{t_f} \{q[L,t;T_1(t)] - Y_{qL}(t)\} \cdot \Delta q[L,t;d^k(t)] \cdot dt}{\int_0^{t_f} \{\Delta q[L,t;d^k(t)]\}^2 \cdot dt} \tag{20}$$

2.4.2 Case II

For this case, the mathematical expression of the sensitivity problem is almost the same as that in Eqs. (14) ~ (17) except that the boundary conditions at x=0 is changed to:

$$-k \frac{\partial \Delta T(0,t)}{\partial x} = \Delta q_1(t) \qquad \text{at } x = 0, \text{ for } t > 0 \tag{21}$$

The search step size β^k for this case can be obtained by replacing $T_1(t)$ with $q_1(t)$ in Eq. (20).

2.5 Adjoint problem and gradient equation

2.5.1 Case I

To obtain the adjoint problem, Eqs. (1) ~ (4) is multiplied by the Lagrange multiplier $\lambda(x,t)$ and the resulting expression is integrated over the correspondent space and time domains. Then the result is added to the right-hand side of Eq. (9) to yield the following expression for the function

$$\begin{aligned} S[T_1(t)] &= \int_0^{t_f} \{Y_{qL}(t) - q[L,t;T_1(t)]\}^2 dt \\ &+ \int_0^{t_f} \int_0^L \lambda(x,t)\left[k \frac{\partial^2 T}{\partial x^2} - \rho c_p \frac{\partial T}{\partial t}\right] dx dt \end{aligned} \tag{22}$$

The variation ΔS is obtained by perturbing T_1 by ΔT_1, T by ΔT and q by Δq in Eq. (22), subtracting from the resulting expression the original Eq. (22) and neglecting the second-order terms, one finds

$$\Delta S[T_1(t)] = \int_0^{t_f}\int_0^{L} 2\{Y_{qL}(t) - q[x,t;T_1(t)]\}\cdot\Delta q(x,t)\cdot\delta(x-L)dxdt + \int_0^{t_f}\int_0^{L}\lambda(x,t)[k\frac{\partial^2\Delta T}{\partial x^2} - \rho c_p\frac{\partial\Delta T}{\partial t}]dxdt \quad (23)$$

where $\delta(\ )$ is the Dirac delta function. In Eq. (23), the domain integral term is reformulated based on the Green's second identity; the boundary conditions of the sensitivity problem give by Eqs. (16) and (17) are utilized and then ΔS is allowed to go to zero. The vanishing of the integrands containing ΔT leads to the following adjoint problem for the determination of $\lambda(x,t)$:

$$\rho c_p\frac{\partial\lambda}{\partial t} + k\frac{\partial^2\lambda}{\partial x^2} + 2\{q[x,t;T_1(t)] - Y_{qL}(t)\}\cdot\frac{\Delta q[x,t;T_1(t)]}{\Delta T[x,t;T_1(t)]}\cdot\delta(x-L) = 0 \quad \text{in } 0 < x < L, \text{ for } t > 0 \quad (24)$$

$$\lambda(x,t_f) = 0 \qquad \text{in } 0 < x < L, \text{ for } t = t_f \quad (25)$$

$$\lambda(0,t) = 0 \qquad \text{at } x = 0, \text{ for } t > 0 \quad (26)$$

$$\lambda(L,t) = 0 \qquad \text{at } x = L, \text{ for } t > 0 \quad (27)$$

The adjoint problem is different from the standard initial value problems in that the final time conditions at time $t = t_f$ is specified instead of the customary initial condition. However, this problem can be transformed to an initial value problem by the transformation of the time variables as $\tau = t_f - t$.

Finally, the following integral term is left:

$$\Delta S[T_1(t)] = \int_0^{t_f} k\frac{\partial\lambda(0,t)}{\partial x}\cdot\Delta T_1(t)dt \quad (28)$$

From definition [20], the functional increment can be presented as:

$$\Delta S[T_1(t)] = \int_0^{t_f}\nabla S[T_1(t)]\cdot\Delta T_1(t)dt \quad (29)$$

A comparison of Eqs. (28) and (29) leads to the following expression for the gradient of functional $S[T_1(t)]$:

$$\nabla S[T_1(t)] = k\frac{\partial\lambda(0,t)}{\partial x} \quad (30)$$

2.5.2 Case II

The adjoint problem for this case is almost the same as that in Eqs. (24) ~ (27) except for the boundary condition at $x = 0$:

$$-k\frac{\partial\lambda(0,t)}{\partial x} = 0 \qquad \text{at } x = 0, \text{ for } t > 0 \quad (31)$$

The gradient of functional $S[q_1(t)]$ is the same as Eq. (30).

2.6 Stopping criterion

Following the recommendations of the Ref. [3, 4], the discrepancy principle is used as the stopping criterion (for Case I):

$$S[T_1(t)] < \chi \quad (32)$$

where χ denotes the tolerance.

It is assumed that the absolute value of the heat flux residuals may be approximated by:

$$\left|Y_{qL}(t) - q[L,t;T_1(t)]\right| \approx \delta \quad (33)$$

where δ is the standard deviation of the measurements. Substituting Eq. (33) into Eq. (9), the following tolerance χ is obtained:

$$\chi = \delta^2 t_f \quad (34)$$

The stopping criterion is then given by Eq. (32) with χ determined from Eq. (34). The stopping criterion for Cases II can be obtained in a similar way.

3. Computational Procedure

Take Case I as the example, the computational procedure for the solution of this inverse problem using CGM may be summarized as follows.

Suppose an initial guess $T_1^0(t)$ is available for the function $T_1(t)$. Set k = 0 and then:

Step 1. Solve the direct problem given by Eqs. (1) ~ (4) and compute $T(x,t)$ based on $T_1^k(t)$.

Step 2. Check the stopping criterion, Eq. (32). Continue if not satisfied.

Step 3. Solve the adjoint problem given by Eqs. (24) ~ (27) for $\lambda(x,t)$.

Step 4. Compute the gradient of the functional $\nabla S[T_1(t)]$ from Eq. (30).

Step 5. Compute the conjugate coefficient γ^k and direction of descent $d^k(t)$ from Eqs. (13) and (12), respectively.

Step 6. Set $\Delta T_1^k(t) = d^k(t)$ and solve the sensitivity problem given by Eqs. (14)~(17) for $\Delta T(x,t)$.

Step 7. Compute the search step size β^k from Eq. (20).

Step 8. Compute the new estimation for $T_1^{k+1}(t)$ from Eq. (11) and return to Step 1.

One of the advantages of using the conjugate gradient method to solve the inverse problems is that the initial guess (i.e. $T_1^0(t)$ for case I) of the unknown quantities can be chosen arbitrarily. In all the simulation cases considered in this study, the initial guess is taken as zero for convenience.

4. Results and Discussion

4.1 Generation of measurement data

In the inverse problems considered in this study, the estimation of the front surface heating condition is based on the measured data at back surface. The measured temperature and heat flux at back surface are generated based on the numerical simulation of the following direct problem:

$$\rho c_p \frac{\partial T}{\partial t} = \frac{\partial}{\partial x}\left(k \frac{\partial T}{\partial x}\right) \qquad \text{in } 0 < x < L, \text{ for } t > 0 \tag{35}$$

$$T(x,0) = T_0 \qquad \text{in } 0 < x < L, \text{ for } t = 0 \tag{36}$$

$$-k \frac{\partial T(L,t)}{\partial x} = q'' - h(T - T_\infty) - \varepsilon\sigma(T^4 - T_\infty^4) \quad \text{at } x = 0, \text{ for } t > 0 \tag{37}$$

$$-k \frac{\partial T(L,t)}{\partial x} = h(T - T_\infty) + \varepsilon\sigma(T^4 - T_\infty^4) \quad \text{at } x = L, \text{ for } t > 0 \tag{38}$$

where q'' is the periodic heat flux imposed at front surface; h is the convection heat transfer coefficient at front and back surfaces, T_∞ is the ambient temperature, ε is the surface emissivity, and σ is the Stefan-Boltzmann constant. This direct problem is numerically solved by the computer code that has been verified in our previous work [21].

By solving Eqs. (35) ~ (38), the heat fluxes and temperatures at both front and back surfaces can be obtained. The front surface temperature and heat fluxes will be used as exact solutions to examine the accuracy of the inverse heat conduction algorithm. The back surface temperature and heat fluxes will be used as boundary condition and employed in objective function, respectively.

Real measurements generally contain errors. We assume normally distributed uncorrelated errors with zero mean and constant standard deviation. Therefore, measurements contain random errors are simulated by adding a random noise (error term) in the form:

$$Y(t) = Y_{exact}(t) + \omega\delta \tag{39}$$

where $Y(t)$ is the simulated experimental data that are obtained from the solution of the direct problem, Eqs. (35) ~ (38); δ is the standard deviation of the measurements. In this study, δ is set as a percentage of the highest measurement value at the back surface; ω is a random variable between 0 and 1 generated by the Mersenne Twister method [22].

4.2 Results of direct problem

In the following simulations, the following thermal properties will be used: ρ = 7600 kg/m^3, c_p = 550 J/(kg•K), k = 18 W/(m•K). Other parameters are: L = 2.5 mm, T_0 = 300 K, T_∞ =300 K, h =5 W/(m^2 • K), and $\varepsilon = 0.92$. The front surface heat flux is assumed to be $q'' = q_c + 0.1q_c \sin(2\pi ft)$ (W/m^2), where q_c is a constant heat flux, which represents the heat flux intensity level at the front surface, and f is the frequency of the sinusoidal component. This type of heat flux is intentionally used to represent a general periodic heating condition although traditional lasers usually have a Gaussian or flat beam profile in time. Unless specified otherwise, the following simulation parameters will be used: heat flux intensity level q_c = 200 W/cm^2, frequency of the sinusoidal component f = 1.0 Hz, standard deviation of the heat flux measurements $\delta = 1\% \cdot [Y_{qL}(t)]_{\max}$. It is assumed that there are no errors in the temperature measurements ($Y_{TL}(t)$).

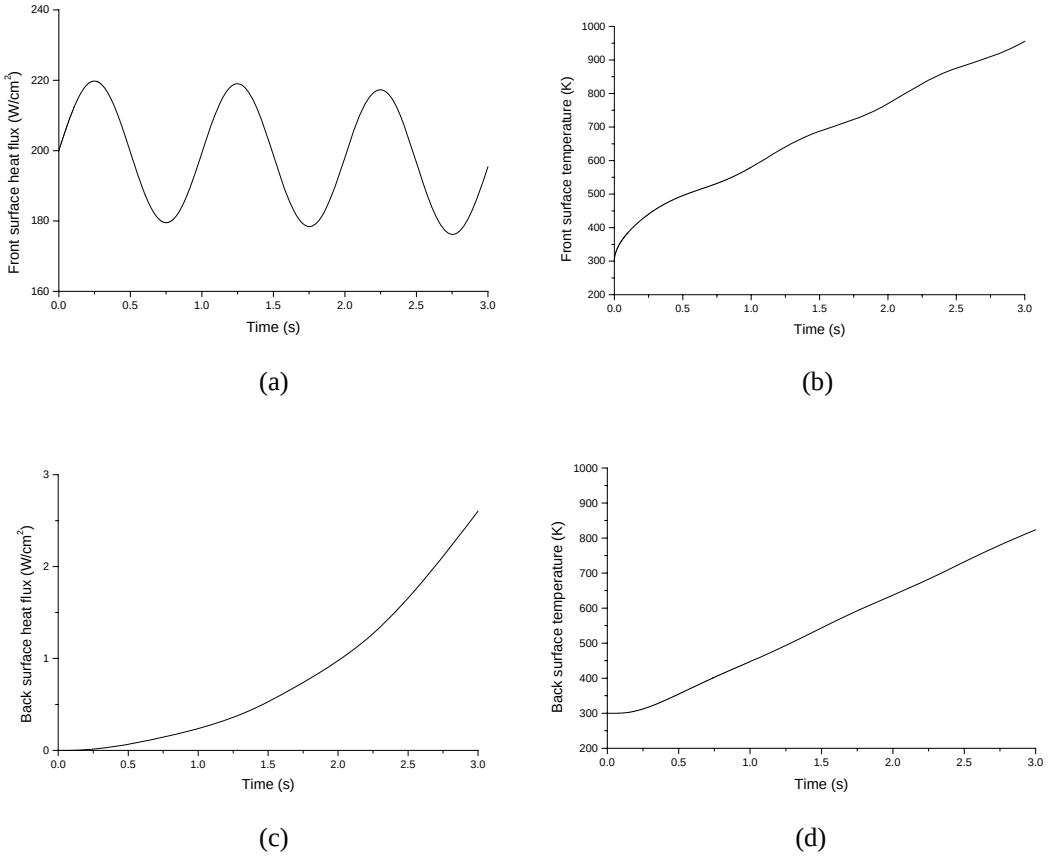

Figure 2 Calculating results for the direct problem described by Eqs.(35)~(38). (a) Front surface heat flux; (b) Front surface temperature; (c) Back surface heat flux; (d) Back surface temperature.

Figure 2 shows the results for the direct problem described by Eqs. (35) ~ (38). It can be seen from Fig. 2(b) that there are some fluctuations in the front surface temperature because the front surface is subjected to a sinusoidal heat flux heating. However, no fluctuations are observed in the back surface heat flux (Fig. 2(c)) and temperature (Fig. 2(d)) due to damp and delay effects in heat diffusion phenomena. In Fig. 2, it seems that the final simulation time t_f is 3.0 s. But the actual final time is taken as t_f = 3.6 s. The reason is as follows. For the conjugate gradient method, the gradient equation is null for some cases at the final time. Under this situation, the initial guess used for $T_1(t)$ or $q_1(t)$ is never changed by the iterative procedure, generating instabilities on the solution in the

neighborhood of t_f . One approach to overcome such difficulties is to consider a final time longer than that of interest [4]. Therefore, we use t_f =3.6 s for the simulations in Fig. 2.

4.3 Comparison between Cases I and II

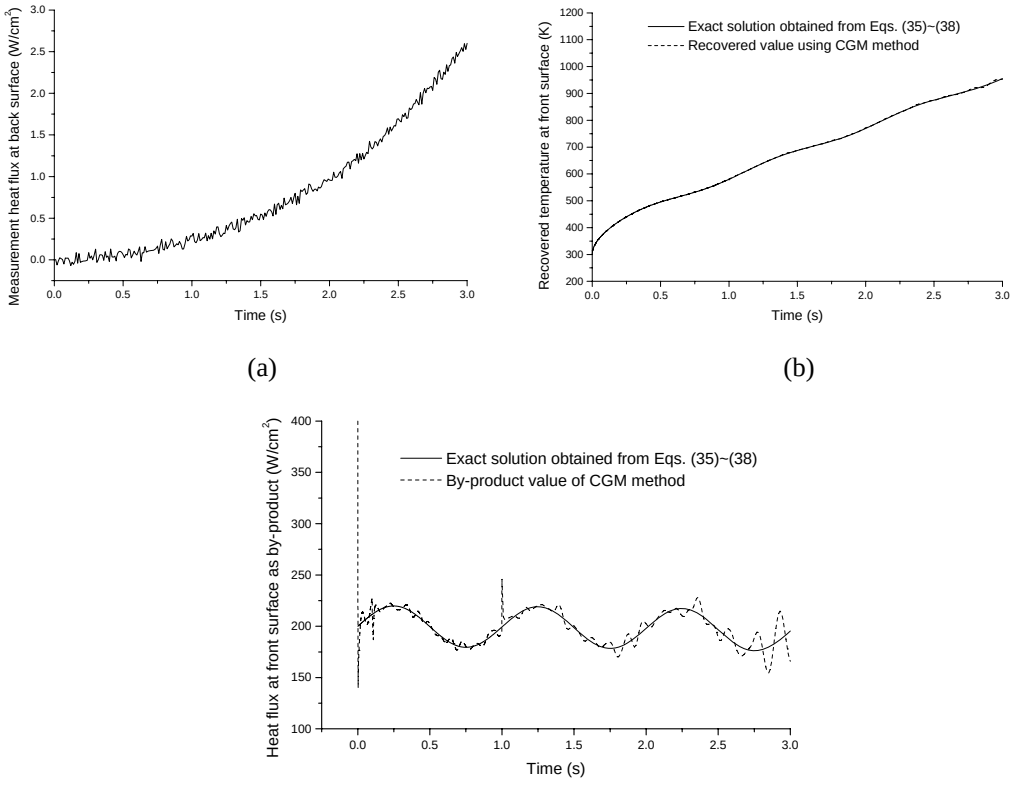

Figure 3 Calculating results for Case I. (a) Back-surface heat flux measurements (with 1% measurement errors); (b) Estimated front-surface temperature by CGM inverse method; (c) Front-surface heat flux as a by-product.

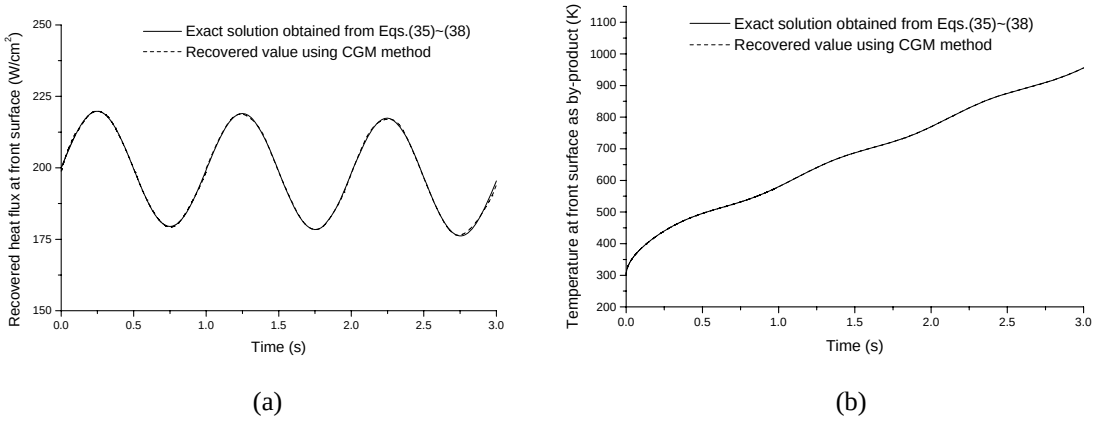

Figure 4 Calculating results for Case II. (b) Estimated front-surface heat flux by CGM inverse method; (c) Front-surface temperature as a by-product.

Figure 3 shows the results for Case I. Fig. 3 (a) gives the measurement heat flux at the back surface obtained by adding 1% random error via Eq. (39). As is seen in Fig. 3(b), the recovered temperature at front surface agrees very well with the exact solution obtained from the solution of Eqs. (35) ~ (38). But the estimation of the front surface heat flux as a byproduct of the CGM algorithm is not satisfactory since there are very large fluctuations around time $t = 0$.

Figure 4 shows the calculating results for Case II. The measured heat flux at back surface has the same error (1%) as in Fig. 3 and therefore is not shown here. It is seen from Fig. 4 that both the recovered temperature and the byproduct heat flux at front surface are in excellent agreement with the exact solutions. Therefore, compared to Case I, Case II provides the most robust numerical scheme for the inverse estimation of the front-surface heating condition based on the measurement data at the back surface. It should be pointed out that the no prior information about the front heating condition is required in the CGM algorithm used in this study.

4.4 Parametric Study for Case II

A powerful numerical scheme for inverse heat transfer should be insensitive to the random measurement errors since the real measurement uncertainties may become very large. Figure 5 presents the effect of heat flux measurement error on the accuracy of the IHCP formulation described by Case II. The simulation parameters are almost the same as those in Fig. 4 except for the random error on the measured heat flux. It can be seen from Fig. 5 (b) that when the heat flux measurement error is increased to 10%, the front surface heat flux can still be reconstructed with a good accuracy. The front surface temperature can be recovered with excellent accuracy (Fig. 5(c)). Clearly, the IHCP formulation of case II proposed in this study is insensitive to measurement errors.

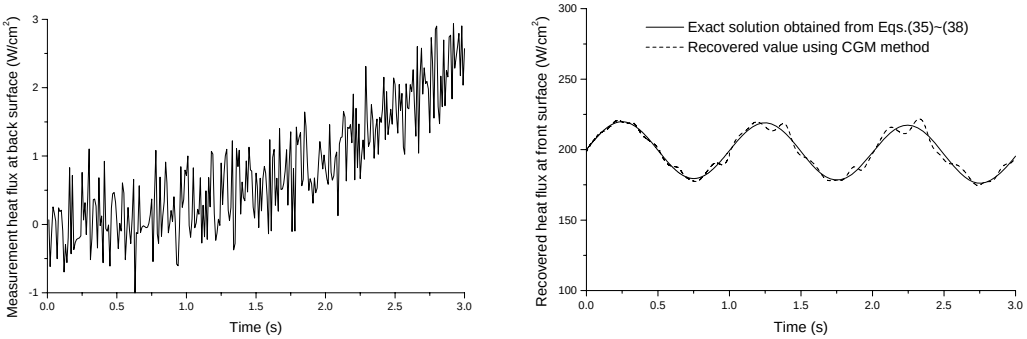

(a) (b)

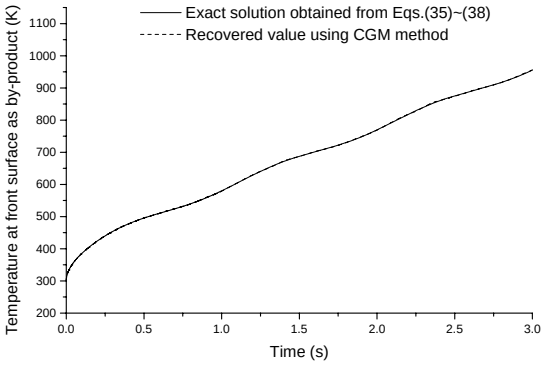

(c)

Figure 5 Effect of heat flux measurement error on the recovery accuracy for Case II. (a) Back-surface heat flux measurements (with 10% measurement errors); (b) Estimated front-surface heat flux by CGM inverse method; (c) Front-surface temperature as a by-product.

Figure 6 presents the effect of the frequency of the sinusoidal component on the recovery accuracy of the IHCP formulation involved in Case II. The simulation parameters are almost the same as those in Fig. 4 except for the frequency of the sinusoidal component. It is found from Fig. 6(a) that when the frequency f is increased to 5 Hz, the phase of the estimated heat flux agrees well with that of the exact solutions, and there is a little decrease in the accuracy of the magnitude of the recovered heat flux signal. Again, the front surface temperature can be recovered with excellent accuracy as a by-product of the inverse algorithm (Fig. 6(b)).

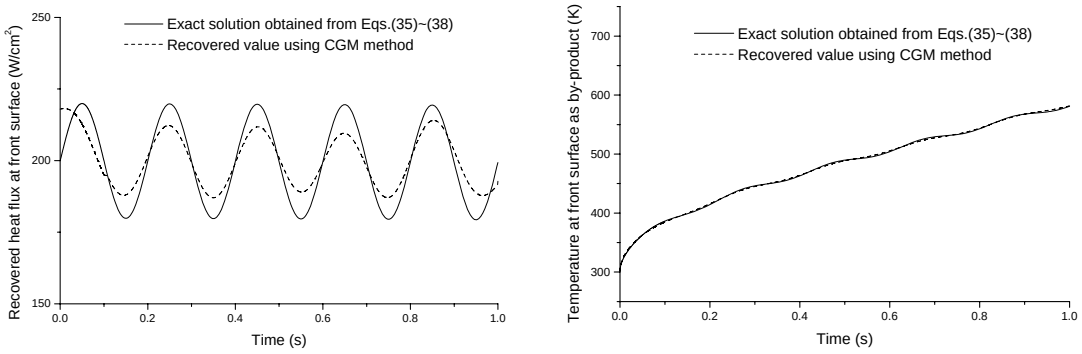

(a) (b)

Figure 6 Effect of frequency of sinusoidal component on the recovery accuracy for Case II (f = 5 Hz). (a) Estimated front-surface heat flux by CGM inverse method; (b) Front-surface temperature as a by-product.

5. Conclusions

A conjugate gradient method (CGM) algorithm is proposed to reconstruct the heat flux and temperature at the front surface of a finite slab which is subjected to high-intensity heating. To achieve high recovery accuracy, both temperature and heat flux are measured at the back surface. The temperature measurement data is used as the back surface boundary condition whereas the heat flux is employed in the objective function. Two cases are examined in detail: I) the front surface temperature is chosen as the unknown to be recovered; II) the front surface heat flux is chosen as the unknown to be recovered. The sensitivity problems and adjoint problems for the two cases are derived and formulated. A CGM iterative numerical procedure is established aiming to obtain a convergent IHCP solution. The results showed that a better accuracy on the recovered front surface boundary condition can be obtained when the front surface heat flux is chosen as the unknown to be recovered (Case II). Consequently, the front surface heat flux – instead of front surface temperature – should be recovered when both back surface temperature and heat flux are known.

The robustness of the suggested IHCP formulation (Case II) is tested for many different cases and it is found that the accuracy of the suggested IHCP formulation is insensitive to heat flux measurement error and can handle periodic front-surface heating fluxes with different frequencies. The work presented in this paper suggests a robust IHCP formulation and provides a guideline for the optimal experimental design in manufacturing and heat treatment.

Acknowledgments

The work presented in this article was funded by the US Army Program Executive Office for Simulation, Training, & Instrumentation under Project No. W900KK-08-C-002 directed by Amit Kapadia and Minh Vuong. The authors would like to express their gratitude to Dr. James L. Griggs for his valuable discussions.

References

[1] dell'Erba, M., Galantucci, L. M., and Miglietta, S., "An Experimental Study on Laser Drilling and Cutting of Composite Materials for the Aerospace Industry Using Excimer and CO_2 Sources," *Composites Manufacturing*, Vol.3, No.1, 1992, pp. 14-19.

[2] Beck, J. V., Blackwell, B., and St-Clair, C. R., *Inverse Heat Conduction: Ill Posed Problems*, Wiley, New York, 1985.

[3] Alifanov, O. M., *Inverse Heat Transfer Problems*, Springer-Verlag, Berlin/Heidelberg, 1994.

[4] Özisik, M. N., and Orlande, H. R. B., *Inverse Heat Transfer: Fundamentals and Applications*, Taylor & Francis, New York, 2000.

[5] Diller, T. E., "Advances in heat flux measurements," *Advances in Heat Transfer*, Vol. 23, 1993, pp. 279-368.

[6] Childs, P. R. N., Greenwood, J. R., and Long, C. A., "Heat flux measurement techniques," *Proceedings of the Institute of Mechanical Engineers. Part C: Journal of Mechanical Engineering Science*, Vol. 213, No. C7, 1999, pp. 655-677.

[7] Tong, A., "Improving the accuracy of temperature measurements," *Sensor Review*, Vol. 21, No. 3, 2001, pp. 193-198.

[8] Childs, P. R. N., "Advances in temperature measurement," *Advances in Heat Transfer*, Vol. 36, 2002, pp. 111-181.

[9] Saidi, A., and Kim, J., "Heat flux sensor with minimal impact on boundary conditions," *Experimental Thermal and Fluid Science*, Vol. 28, 2004, pp. 903-908.

[10] Loulou, T., and Scott, E. P., "An inverse heat conduction problem with heat flux measurements," *International Journal for Numerical Methods in Engineering*, Vol. 67, 2006, pp. 1587-1616.

[11] Sparrow, E. M., Haji-Sheikh, A., and Lundgren, T. S., "The inverse problem in transient heat conduction," *ASME Journal of Applied Mechanics*, Vol.86, 1964, pp. 369-375.

[12] Jarny, Y., Özisik, M. N., and Bardon, J. P., "A general optimization method using adjoint equation for solving multidimensional inverse heat conduction," *International Journal Heat and Mass Transfer*, Vol.34, 1991, pp. 2911-2919.

[13] Pasquetti, R., Niliot, C. L., "Boundary element approach for inverse heat conduction problems: application to a bidimensional transient numerical experiment," *Numerical Heat Transfer, Part B*, Vol. 20, 1991, pp. 169-189.

[14] Yang, C. -Y. , and Chen, C. –K., "The boundary estimation in two-dimensional inverse heat conduction problems," *Journal of Physics D: Applied Physics*, Vol. 29, 1996, pp. 333-339.

[15] Huang, C. –H, and Wang, S. –P., "A three-dimensional inverse heat conduction problem in estimating surface heat flux by conjugate gradient method," *International Journal of Heat and Mass Transfer*, Vol. 42, 1999, pp. 3387-3403.

[16] Emery, A. F., Nenarokomov, A. V., and Fadale, T. D., "Uncertainties in parameter estimation: the optimal experimental design," *International Journal of Heat and Mass Transfer*, Vol. 43, 2000, pp. 3331-3339.

[17] Monde, M., Arima, H., and Mitsutake, Y., "Estimation of surface temperature and heat flux using inverse solution for one-dimensional heat conduction," *ASME Journal of Heat Transfer*, Vol. 125, 2003, pp. 213-223.

[18] Xue, X., Luck, R., and Berry, J. T., "Comparisons and improvements concerning the accuracy and robustness of inverse heat conduction algorithms," *Inverse Problems in Science and Engineering*, Vol. 13, No. 2, 2005, pp. 177-199.

[19] Frankel, J. I., Osborne, G. E., and Taira, K., "Stabilization of ill-posed problems through thermal rate sensors," *AIAA Journal of Thermophysics and Heat Transfer*, Vol. 20, No. 2, 2006, pp. 238-246.

[20] Alifanov, O. M., "Solution of an inverse problem of heat conduction by iteration methods," *Journal of Engineering Physics*, Vol. 26, 1974, pp. 471-476.

[21] Zhou, J., Zhang, Y., Chen, J. K., and Smith, D. E., "A nonequilibrium thermal model for rapid heating and pyroloysis of organic composites," *ASME Journal of Heat Transfer*, Vol. 130, 2008, 064501.

[22] Matsumoto, M., and Nishimura, T., "Mersenne Twister: a 623-dimensionally equidistributed uniform pseudorandom number generator," *ACM Transactions on Modeling and Computer Simulation*, Vol.8, No.1, 1998, pp. 3-30.